Crystal Structures and Magnetic Properties of New Cyano-Bridged Two-Dimensional Grid-Like Bimetallic Assemblies $[Ni(tn)_2]_2[Cr(CN)_5((NO)]OH\cdot H_2O$ and $[Ni(tn)_2]_2[Co(CN)_6]NO_3\cdot 2H_2O$ (tn = 1,3-Propanediamine)

Hui-Zhong Kou,[†,#] Jin-Kui Tang,[†] Dai-Zheng Liao,*[,†] Song Gao,[§] Peng Cheng,[†] Zong-Hui Jiang,[†] Shi-Ping Yan,[†] Geng-Lin Wang,[†] Benoît Chansou,[‡] and Jean-Pierre Tuchagues[‡]

Department of Chemistry, Nankai University, Tianjin 300071, P.R. China, State Key Laboratory of Rare Earth Materials Chemistry and Applications, Peking University, Beijing 100871, P. R. China, and Laboratoire de Chimie de Coordination, UPR CNRS 8241, 205 route de Narbonne, 31077 Toulouse, France

Received November 28, 2000

Two bimetallic assemblies, $[Ni(tn)_2]_2[Cr(CN)_5(NO)]OH\cdot H_2O$ (**1**) and $[Ni(tn)_2]_2[Co(CN)_6]NO_3\cdot 2H_2O$ (**2**) (tn = 1,3-diaminopropane), have been prepared and structurally and magnetically characterized. Crystal data for **1** (**2**): space group $P\bar{1}$ ($P\bar{1}$), $a = 8.698(3)$ (8.937(2)) Å, $b = 10.001(2)$ (9.863(1)) Å, $c = 10.158(2)$ (10.064(1)) Å, $\alpha = 87.40(2)$ (86.064(10))°, $\beta = 65.10(2)$ (65.489(10))°, $\gamma = 81.63(2)$ (81.572(12))° and $Z = 1$ (1). Both structures consist of two-dimensional grid-like polycations containing Ni−N≡C−M linkages (M = Cr or Co) and counteranions (OH, NO_3). Magnetic studies of **1** showed that the complex displays a metamagnetic behavior originating from intralayer ferromagnetic and interlayer antiferromagnetic interactions. Long-range antiferromagnetic ordering was observed at $T_N = 3.3$ K. Complex **2** exhibits intramolecular ferromagnetic interactions through the diamagnetic N≡C−Co−N≡C bridges, owing to superexchange involving the empty d_σ orbital of the diamagnetic Co(III) ion.

Introduction

Coordination polymers derived from metal cyanides have attracted great attention due to their potential use as functional solid materials, such as catalysts, optical devices as well as molecule-based magnets.[1−33] The synthetic strategy consists of building zero-, one-, two- and three-dimensional assemblies from hexacyanometalate(II, III, IV) and transition metal-ion building blocks. In the case of 3-D Prussian blue analogues of general formula $M_x[M'(CN)_6]_y\cdot nH_2O$,[2−12] magnetic ordering has been observed above room temperature.[6] Inducing controlled modi-

* To whom correspondence should be addressed.
[†] Nankai University.
[#] Present address: Department of Chemistry, Tsinghua University, Beijing 100087, P. R. China.
[§] Peking University.
[‡] Laboratoire de Chimie de Coordination.

(1) Dunbar, K. R.; Heintz, R. A. *Prog. Inorg. Chem*. **1997**, 283.
(2) (a) Herren, F.; Fischer, P.; Ludi, A.; Hälg, W. *Inorg. Chem*. **1980**, *19*, 956. (b) Klenze, R.; Kanellakopulos, B.; Trageser, G.; Eysel, H. H. *J. Chem. Phys*. **1980**, *72*, 5819.
(3) (a) Griebler, W. D.; Babel, D. *Z. Naturforsch*., Teil. B **1982**, *87*, 832. (b) Buschmann, W. E.; Ensling, J.; Gütlich, P.; Miller, J. S. *Chem. Eur. J*. **1999**, *5*, 3019.
(4) Gadet, V.; Mallah, T.; Castro, I.; Verdaguer, M. *J. Am. Chem. Soc*. **1992**, *114*, 9213.
(5) Mallah, T.; Thiebaut, S.; Verdaguer, M.; Veillet, P. *Science* **1993**, *262*, 1554.
(6) (a) Holmes, S. M.; Girolami, G. S. *J. Am. Chem. Soc*. **1999**, *121*, 5593. (b) Hatlevik, *ϕ*.; Buschmann, W. E.; Zhang, J.; Manson, J. L.; Miller, J. S. *Adv. Mater*. **1999**, *11*, 914.
(7) (a) Entley, W. R.; Girolami, G. S. *Inorg. Chem*. **1994**, *33*, 5165. (b) Ferlay, S.; Mallah, T.; Ouahes, R.; Veillet, P.; Verdaguer, M. *Inorg. Chem*. **1999**, *38*, 229.
(8) Entley, W. R.; Girolami, G. S. *Science* **1995**, *21*, 268.
(9) Ferlay, S.; Mallah, T.; Ouaches, R.; Veillet, P.; Verdaguer, M. *Nature* **1995**, *378*, 701.
(10) (a) Sato, O.; Iyoda, T.; Fujishima, A.; Hashimoto, K. *Science* **1996**, *271*, 49. (b) Sato, O.; Iyoda, T.; Fujishima, A.; Hashimoto, K. *Science* **1996**, *272*, 704.
(11) Holmes, S. M.; Girolami, G. S. *Mol. Cryst. Liq. Cryst. A* **1997**, *305*, 279.
(12) (a) Larionova, J.; Sanchiz, J.; Golhen, S.; Ouahab, L.; Kahn, O. *Chem. Commun*. **1998**, 953. (b) Larionova, J.; Kahn, O.; Golhen, S.; Ouahab, L.; Clerac, R. *J. Am. Chem. Soc*. **1998**, *120*, 13088.
(13) (a) Zhong, Z. J.; Seino, H.; Mizobe, Y.; Hidai, M.; Fujishima, A.; Ohkoshi, S.; Hashimoto, K. *J. Am. Chem. Soc*. **2000**, *122*, 2952. (b) Rogez, G.; Marvilliers, A.; Riviere, E.; Audiere, J. P.; Lloret, F.; Varret, F.; Goujon, A.; Mendenez, N.; Girerd, J. J.; Mallah, T. *Angew. Chem., Int. Ed*. **2000**, *39*, 2885.
(14) Langenberg, K. V.; Batten, S. R.; Berry, K. J.; Hockless, D. C. R.; Moubaraki, B.; Murray, K. S. *Inorg. Chem*. **1997**, *36*, 5006.
(15) Smekal, Z.; Travnicek, Z.; Marek, J.; Nadvornik, M. *Aust. J. Chem*. **2000**, *53*, 225.
(16) (a) Ohba, M.; Maruone, N.; Okawa, H.; Enoki, T.; Latour, J.-M. *J. Am. Chem. Soc*. **1994**, *116*, 11566. (b) Ohba, M.; Fukita, N.; Okawa, H. *J. Chem. Soc., Dalton Trans*. **1997**, 1733. (c) Ohaba, M.; Usuki, N.; Fukita, N.; Okawa, H. *Inorg. Chem*. **1998**, *37*, 3349.
(17) (a) Zou, J. Z.; Hu, X. D.; Duan, C. Y.; Xu, Z.; You, X. Z.; Mak, T. C. W. *Transition Met. Chem*. **1998**, *23*, 477. (b) Colacio, E.; Dominguez-Vera, J. M.; Ghazi, M.; Kivekas, R.; Moreno, J. M.; Pajunen, A. *J. Chem. Soc., Dalton Trans*. **2000**, 505. (c) Marvillers, A.; Parsons, S.; Riviere, E.; Audiere, J.-P.; Mallah, T. *Chem. Commun*. **1999**, 2217.
(18) (a) Kou, H.-Z.; Liao, D.-Z.; Cheng, P.; Jiang, Z.-H.; Yan, S.-P.; Wang, G.-L.; Yao, X.-K.; Wang, H.-G. *J. Chem. Soc., Dalton Trans*. **1997**, 1503. (b) Fu, D. G.; Chen, J.; Tan, X. S.; Jiang, L. J.; Zhang, S. W.; Tang, W. X. *Inorg. Chem*. **1997**, *36*, 220. (c) Ferbinteanu, M.; Tanase, S.; Andruh, M.; Journaux, Y.; Cimpoesu, F.; Strenger, I.; Riviere, E. *Polyhedron* **1999**, *18*, 3019.
(19) (a) Colacio, E.; Dominguez-Vera, J.; Ghazi, M. M.; Kivekas, R.; Klinga, M.; Moreno, J. M. *Chem. Commun*. **1998**, 1071. (b) Matsumoto, N.; Sunatsuki, Y.; Miyasaka, H.; Hashimoto, Y.; Luneau, D.; Tuchagues, J.-P. *Angew. Chem., Int. Ed. Engl*. **1999**, *38*, 171. (c) Miyasaka, H.; Matsumoto, N.; Re, N.; Gallo, E.; Floriani, C. *Inorg. Chem*. **1997**, *36*, 670.

10.1021/ic0013330 CCC: $20.00
Published on Web 08/07/2001

fications in the topology of the complexes through incorporation of organic ligands allows a better understanding of the magneto-structural correlations.[13−33]

To build new molecule-based magnetic materials it is desirable to explore alternative building blocks containing cyanide groups. Recently, Holmes and Girolami[11] have initiated studies on some Prussian blue analogues containing $[Cr(CN)_5(NO)]^{3-}$. On the basis of powder XRD analysis, these authors found that the ferrimagnetic complex $K_{0.5}Mn[Cr(CN)_5(NO)]_{0.83}\cdot 4H_2O\cdot 1.5MeOH$ has a cubic structure; on the basis of the N═O stretching frequency which is ca. 60 cm^{-1} higher than in $K_3[Cr(CN)_5(NO)]$ (1630 cm^{-1}), the NO^+ group is bridging. On the basis of a single-crystal X-ray diffraction analysis, we have observed that the 2-D honeycomblike assembly $[NiL]_3[Cr(CN)_5(NO)]_2\cdot 10H_2O$ (L = 3,10-dimethyl-1,3,6,8,10,12-hexaazacyclooctadecane) exhibits ferromagnetic ordering at 4.5 K and that the NO^+ group does not participate in bridging.[26b] To gain further evidence on the binding modes of $[Cr(CN)_5(NO)]^{3-}$ with transition metal complexes, we have studied the reaction of $[Ni(tn)_3]^{2+}$ (tn = 1,3-propanediamine) with $[Cr(CN)_5(NO)]^{3-}$, and obtained a novel two-dimensional grid-like assembly, $[Ni(tn)_2]_2[Cr(CN)_5(NO)]OH\cdot H_2O$ (**1**). With the aim of determining the factors which control the magnetic properties, we have also prepared and magnetically investigated the complex $[Ni(tn)_2]_2[Co^{III}(CN)_6]NO_3\cdot 2H_2O$ **2**: a marked ferromagnetic behavior has been observed. In this contribution, we describe the synthesis, characterization, X-ray crystal structure, and magnetic properties of complexes **1** and **2**.

Experimental Section

Materials and Syntheses. All reagents used in the syntheses were of analytical grade and used without further purification. The $K_3[Cr(CN)_5(NO)]\cdot H_2O$ and $K_3[Co(CN)_6]$ precursors were prepared according to literature methods.[34,35]

Preparation of $[Ni(tn)_2]_2[Cr(CN)_5(NO)]OH\cdot H_2O$ (1). To an aqueous solution of $Ni(tn)_3(NO_3)_2$ prepared by mixing $Ni(NO_3)_2\cdot 6H_2O$ (1 mmol, 290.8 mg) and tn (3 mmol, 222.3 mg) in 20 mL of water, $K_3[Cr(CN)_5(NO)]\cdot H_2O$ (0.5 mmol, 165 mg) in water (15 mL) was added at room temperature. Yellow microcrystals immediately precipitated, which were collected by suction filtration, washed with water and ethanol, and dried *under vacuum* over P_2O_5. Yield: 253.3 mg, 80%. Anal. Calc for $C_{17}H_{43}N_{14}O_3CrNi_2$: C, 30.89; H, 6.56; N, 29.67%. Found: C, 31.32; H, 6.39; N, 30.04. IR (KBr): $\nu_{C\equiv N}$ 2140 and 2110 cm^{-1}; $\nu_{N=O}$ 1665 cm^{-1}. Yellow single crystals of $\mathbf{1}\cdot C_2H_5OH$ suitable for X-ray diffraction analysis were obtained by slow evaporation in a refrigerator of a reaction mixture including a tn excess (Ni/tn = 1:10) and a small amount of ethanol.

$[Ni(tn)_2]_2[Co(CN)_6]NO_3\cdot 2H_2O$ (2). To an aqueous solution of $Ni(tn)_3(NO_3)_2$ prepared in situ by mixing $Ni(NO_3)_2\cdot 6H_2O$ (1 mmol, 290.8 mg) and tn (3 mmol, 222.3 mg) in 20 mL of water, $K_3[Co(CN)_6]$ (0.5 mmol, 166 mg) in water (15 mL) was added at room temperature. Violet microcrystals precipitated from the resulting violet solution within 10 min. They were collected by suction filtration, washed with water, and dried *under vacuum* over P_2O_5. Yield: 254 mg, 70%. Anal. Calcd. for $C_{18}H_{44}N_{15}O_5CoNi_2$: C, 29.74; H, 6.10; N, 28.90. Found: C, 30.16; H, 5.88; N, 28.43%. IR (KBr): $\nu_{C\equiv N}$ 2150 and 2145 cm^{-1}; ν_{O-N} (NO_3-) 1382 cm^{-1}. Violet crystals suitable for X-ray single-crystal structure analysis were obtained by slow evaporation of the above filtrate in a refrigerator.

Physical Measurements. C, H, and N elemental analyses were carried out with a Perkin-Elmer analyzer model 240. IR spectra were recorded on a 5DX FT-IR spectrophotometer in the 4000−400 cm^{-1} range. Samples were run as KBr pellets. Variable-temperature magnetic susceptibility (1.8−300 K for **1** and 1.8−200 K for **2**) in a 1 T magnetic field, zero-field ac magnetic susceptibility (1.9−10.6 K) and magnetization (0 to ±0.2 T and 0−6 T at 1.93 K) measurements were performed on a Maglab System^{2000} magnetometer. The experimental susceptibilities were corrected for the diamagnetism of constituent atoms (Pascal's Tables).

X-ray Structure Determinations. The selected crystal was pasted on a glass fiber and mounted on a Stoe Imaging Plate Diffraction System (IPDS) equipped with an oxford cryostream cooler device (**1**) and a Siemens *P*4 diffractometer (**2**), both using a graphite-monochromated Mo Kα radiation (=0.71069 Å). The data were collected at 180 K (**1**) and 293 K (**2**). Final unit cell parameters were obtained by least-squares refinement of a set of 5000 reflections for **1**, and of the setting angles of 25 reflections with $10.0° < \theta < 15.0°$ for **2**. The crystal decay was monitored by measuring 200 reflections per image (**1**), and three standard reflections every 2 h (**2**). No significant fluctuations of diffracted intensities were observed during the measurements. A total of 5956 (**1**) and 3400 (**2**) reflections were collected, of which 1730 (**1**) and 2593 (**2**) were considered observed and used in the structure refinements. The structures were solved by direct methods using SIR92[36] (**1**) and SHELXS-93 (**2**) and refined by least-squares procedures on F_o (**1**) with CRYSTALS[37] and on F_o^2 (**2**) with SHELXL-93 by minimizing

(20) (a) Kou, H.-Z.; Wang, H.-M.; Liao, D.-Z.; Cheng, P.; Jiang, Z.-H.; Yan, S.-P.; Huang X.-Y.; Wang, G.-L. *Aust. J. Chem*. **1998**, *51*, 661. (b) Kou, H.-Z.; Liao, D.-Z.; Jiang, Z.-H.; Yan, S.-P.; Wu, Q.-J.; Gao, S.; Wang, G.-L. *Inorg. Chem. Commun.* **2000**, *3*, 153. (c) Shu, H. L.; Wei, H. H.; Wang, Y. *Inorg. Chim. Acta* **1997**, *258*, 81. (d) Zhan, S.-Z.; Guo, D.; Zhang, X.-Y.; Du, C.-X.; Zhu, Y.; Yang, R.-N. *Inorg. Chim. Acta* **2000**, *298*, 57.

(21) Smith, J. A.; Galan-Mascaros, J.-R.; Clerac, R.; Dunbar, K. R. *Chem. Commun*. **2000**, 1077.

(22) (a) Ohba, M.; Okawa, H.; Ito, T.; Ohto, A. *J. Chem. Soc., Chem. Commun*. **1995**, 1545. (b) Ohba, M.; Okawa, H.; Fukita, N.; Hashimoto, Y. *J. Am. Chem. Soc*., **1997**, *119*, 1011.

(23) Mondal, N.; Saha, M. K.; Bag, B.; Mitra, S.; Gramlich, V.; Ribas, J.; El Fallah, M. S. *J. Chem. Soc., Dalton Trans*. **2000**, 1601.

(24) Kou, H.-Z.; Bu, W.-M.; Liao, D.-Z.; Cheng, P.; Jiang, Z.-H.; Yan, S.-P.; Fan Y.-G.; Wang, G.-L. *J. Chem. Soc., Dalton Trans*. **1998**, 4161.

(25) Ferlay, S.; Mallah, T.; Vaissermann, J.; Bartolome, F.; Veillet, P.; Verdaguer, M. *J. Chem. Soc., Chem. Commun*. **1996**, 2481.

(26) (a) Kou, H.-Z.; Gao, S.; Bu, W.-M.; Liao, D.-Z.; Ma, B.-Q.; Jiang, Z.-H.; Yan, S.-P.; Fan, Y.-G.; Wang, G.-L. *J. Chem. Soc., Dalton Trans*. **1999**, 2477. (b) H.-Z. Kou, S. Gao, B.-Q. Ma, D.-Z. Liao, *Chem. Commun*. **2000**, 713. (c) H.-Z. Kou, S. Gao, B.-Q. Ma, D.-Z. Liao, *Chem. Commun*. **2000**, 1309. (d) Colacio, E.; Domínguez-Vera, J. M.; Ghazi, M.; Kivekäs, R.; Lloret, F.; Moreno, J. M.; Stoeckli-Evans, H. *Chem. Commun*. **1999**, 987. (e) Kou, H.-Z.; Bu, W.-M.; Gao, S.; Liao, D.-Z.; Jiang, Z.-H.; Yan, S.-P.; Fan, Y.-G.; Wang, G.-L. *J. Chem. Soc., Dalton Trans*. **2000**, 2996.

(27) Miyasaka, H.; Ieda, H.; Matsumoto, N.; Re, N.; Crescenzi, R.; Floriani, C. *Inorg. Chem*. **1998**, *37*, 255.

(28) Miyasaka, H.; Matsumoto, N.; Okawa, H.; Re, N.; Gallo, E.; Floriani, C. *Angew. Chem., Int. Ed. Engl*. **1995**, *34*, 1446. Miyasaka, H.; Matsumoto, N.; Okawa, H.; Re, N.; Gallo. E.; Floriani, C. *J. Am. Chem. Soc*. **1996**, *118*, 981.

(29) Re, N.; Gallo, E.; Floriani, C.; Miyasaka. H.; Matsumoto, N. *Inorg. Chem*. **1996**, *35*, 5964.

(30) Re, N.; Crescenzi, R.; Floriani, C.; Miyasaka, H.; Matsumoto, N. *Inorg. Chem*. **1998**, *37*, 2717.

(31) Sra, A. K.; Andruh, M.; Kahn, O.; Golhen, S.; Ouahab, L.; Yakhmi, J. V. *Angew. Chem., Int. Ed. Engl.* **1999**, *38*, 2606.

(32) (a) Larionova, J.; Kahn, O.; Golhen, S.; Ouahab, L.; Clerac, R. *J. Am. Chem. Soc*. **1999**, *121*, 3349. (b) Rombaut, G.; Golhen, S.; Ouahab, L.; Mathoniére, C.; Kahn, O. *J. Chem. Soc., Dalton Trans*., **2000**, 3609. (c) Bernhardt, P. V.; Macpherson, B. P.; Martinez, M. *Inorg. Chem*. **1998**, *37*, 2717.

(33) (a) Zhang, S.-W.; Fu, D.-G. Sun, W.-Y.; Hu, Z.; Yu, K.-B.; Tang, W.-X. *Inorg. Chem*. **2000**, *39*, 1142. (b) El Fallah, M. S.; Rentschler, E.; Caneschi, Sessoli, A.; R.; Gatteschi, D. *Angew. Chem., Int. Ed. Engl*. **1996**, *35*, 1947. (c) Ohba, M.; Usuki, N.; Fukita N.; Okawa, H. *Angew. Chem., Int. Ed. Engl.* **1999**, *38*, 1795. (d) Fukita, N.; Ohba, M.; Okawa, H.; Matsuda K.; Iwamura, H. *Inorg. Chem*. **1998**, *37*, 842.

(34) Griffith, W. P.; Lewis J.; Wilkinson, G. *J. Chem. Soc*. **1959**, 872.

(35) Bertini, I.; Luchinat, C.; Mani, F.; Scozzafava, A. *Inorg. Chem*. **1980**, *19*, 1333.

(36) Altamore, A.; Cascarano, G.; Giacovazzo, G.; Guargliardi, A.; Burla, M. C.; Polidori, G.; Camalli, M. *J. Appl. Crystallogr.* **1994**, *27*, 435

(37) Watkin, D. J.; Carruthers, J. R.; Betteridge, P. W. *CRYSTALS*; Chemical Crystallography Laboratory, University of Oxford: Oxford, 1985.

Table 1. Crystal Parameters for Complexes **1**· and **2**

formula	$C_{19}H_{49}N_{14}O_4CrNi_2$	$C_{18}H_{44}N_{15}O_5CoNi_2$
fw	707.1	727.03
space group	*P*1	*P*1
a/Å	8.698(3)	8.937(2) Å
b/Å	10.001(2)	9.863(1) Å
c/Å	10.158(2)	10.064(1) Å
α/deg	87.40(2)	86.064(10)°
β/deg	65.10(2)	65.489(10)°
γ/deg	81.63(2)	81.572(12)°
Z	1	1
temperature/K	180	293(2)
λ/Å	0.71073	0.71069
ρ (calc) g cm^{-3}	1.29	1.29
μ (Mo Kα)/cm^{-1}	8.17	17.34
R (*F*)	0. 0623	0.0433
R_w	0.0681 (*F*)	0.0558 (F^2)

the functions: $\sum w(||F_o| - |F_c||)^2$ for **1** and $\sum w(F_o^2 - F_c^2)^2$ for **2**, where F_o and F_c are, respectively, the observed and calculated structure factors. The atomic scattering factors were taken from the international tables for X-ray crystallography.[38] All atoms were located on difference Fourier maps. All non-hydrogen atoms were refined anisotropically. H atoms were introduced in calculations with the riding model. A statistical disorder has been found on a ligand connected to the Cr atom of **1**: CN and NO are located at the same site and have been refined with an occupancy factor of 0.5. Occupancy factors for OH, H_2O, and EtOH of **1** were refined to 0.5. The electronic density of EtOH, close to an inversion center, appears as disordered. The three oxygen atoms of the nitrate ion in **2** experience a serious disorder over two positions and were refined with an occupancy factor of 0.5. Weighted *R*-factors *wR* and goodness of fit *S* are based on F_o^2, conventional *R*-factors *R* are based on F_o, with F_o set to zero for negative F_o^2. Crystal data collection and refinement parameters are given in Table 1.

Results

IR Spectra. The IR spectrum of complex **1** shows two strong bands at 2150 and 2110 cm^{-1}, which are attributed to C≡N stretching modes. The shift of (C≡N) to higher wavelength compared with that of $K_3[Cr(CN)_5(NO)]$ (2120 cm^{-1})[39] is characteristic of bridging CN^-, as observed for other cyano-bridged systems. The IR spectrum of **2** shows one sharp band at 2150 and a shoulder at 2145 cm^{-1} in the (C≡N) region. The shift of (C≡N) to higher wavelength compared to $K_3[Co(CN)_6]$ (2119 cm^{-1}) suggests formation of CN^- bridges as revealed by the X-ray structure determination. The appearance of a sharp band at 1382 cm^{-1} in the spectrum indicates the presence of free NO_3^- anions.

Crystal Structures. The asymmetric unit of **1** is shown in Figure 1. Projections of the lattice perpendicular to the *a* axis (showing a layer) and slightly tilted with respect to *a* (showing the stacking of layers) are shown in Figures 2a and b, respectively. Selected bond distances and angles are listed in Table 2. The structure consists of 2-D grid-shaped $\{[Ni(tn)_2]_2[Cr(CN)_5(NO)]\}_n^{n+}$ cationic layers resulting from the cross-linking of −Cr−C≡N−Ni− chains forming an infinite network of $\{-Cr-C\equiv N-Ni-\}_4$ basic units. Each $[Ni(tn)_2]$ unit is linked to two $[Cr(CN)_5(NO)]^{3-}$ complex anions trans to each other. Each nickel(II) cation assumes a slightly distorted octahedral environment with Ni−N bond distances ranging from 2.108(4) to 2.131(5) Å for Ni(1)−N and from 2.102(5) to 2.125(4) Å for Ni(2)−N. Each $[Cr(CN)_5(NO)]^{3-}$ unit is connected to four $[Ni(tn)_2]^{2+}$ complex cations through four C≡N groups in the equatorial plane, whereas the remaining CN^- and NO^+ groups are monodentate. The chromium(I) cation is located at the crystallographic inversion center, and consequently the CN^- and NO^+ groups are statistically disordered. The Cr−C bond distances in the equatorial plane are 2.040(5) and 2.054(6) Å, close to those in the ionic complex $[Co(en)_3][Cr(CN)_5(NO)]\cdot 2H_2O$.[40] The axial Cr−C/N bond distance (1.883(5) Å) is in good agreement with the average value of axial Cr−C (2.075 Å) and Cr−N (1.708 Å) bond distances. The Ni−N≡C bond angles are 148.2(4)° and 153.9(4)°, i.e., the bridging CN ligands coordinate to Ni(II) ions in a bent fashion. The distances between nearest Cr and Ni neighbors are 5.001 Å for Cr···LNi(1) and 5. 078 Å for Cr···LNi(2).

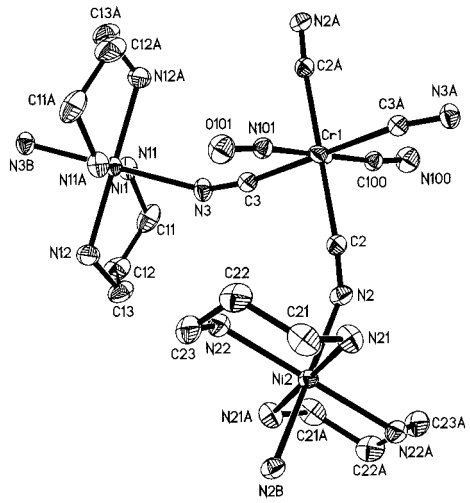

Figure 1. View of complex **1** with atom numbering scheme showing 30% probability ellipsoids (hydrogen atoms are omitted for clarity).

Table 2. Selected Bond Lengths (Å) and Angles (deg) for Complex **1**·

Cr−C(100)/N(101)	1.883(5)	Cr−C(2)	2.054(6)
Cr−C(3)	2.040(5)	Ni(1)−N(11)	2.131(5)
Ni(1)−N(12)	2.109(5)	Ni(1)−N(3)	2.108(4)
Ni(2)−N(21)	2.117(5)	Ni(2)−N(22)	2.125(4)
Ni(2)−N(2)	2.102(5)	C(100)−N(100)	1.180(7)
C(2)−N(2)	1.146(7)	C(3)−N(3)	1.155(7)
Ni(2)−N(2)−C(2)	153.9(4)	Ni(1)−N(3)−C(3)	148.2(4)

The ethanol molecules are situated within the holes of the $\{-Cr-C\equiv N-Ni-\}_4$ basic units of the grid, close to an inversion center, and hydrogen-bonded to the tn molecules (O···LN = 3.038(8) Å). The layers align along [101] with a separation of ca. 8.70 Å, and the interlayer metal−metal distance is 8.698(3) Å for Ni(2)···Ni(2), Ni(1)···Ni(1), and Cr···Cr (cell dimension ***a***). The water molecules and the OH^- counteranion are located between the layers and hydrogen-bonded to the terminal CN^- (NO^+) ligands of $[Cr(CN)_5(NO)]^{3-}$, the nitrogen atom of the tn ligand and other water molecules with O···N and O···O distances ranging from 2.756(8) to 3.038(8) Å.

Complex **2** is nearly isostructural to $[Ni(tn)_2]_2[Fe(CN)_6]NO_3\cdot 2H_2O$.[24] Selected bond distances and angles are listed in Table 3. The structure (Figure 3) consists of two *trans*-$[Ni(tn)_2]^{2+}$ cations, one $Co(CN)_6^{3-}$, one NO_3^- anion and two lattice water molecules. The 2-D grid-like $\{[Ni(tn)_2]_2[Co(CN)_6]\}_n^{n+}$ polycations are formed through Ni−C≡N−Co linkages and can be described as an infinite network of $\{-Ni-C\equiv N-Co-\}_4$ basic units resulting from the cross-linking of Ni−C≡N−Co chains (Figure 4) in a way similar to that described for complex **1** with $\{-Cr-C\equiv N-Ni-\}_4$ basic units. Each hexacyanocobaltate(III)

(38) Ibers, J. A.; Hamilton, W. C. *International Table for X-ray Crystallography*; Kynoch Press: Birmingham, England, 1974; Vol. IV.
(39) Gans, P.; Sabatini, A.; Sacconi, L. *Inorg. Chem*. **1966**, *5*, 1877.
(40) Enemark, J. H.; Quinby, M. S.; Reed, L. L.; Steuck, M. J.; Walthers, K. K. *Inorg. Chem*. **1970**, *9*, 2397.

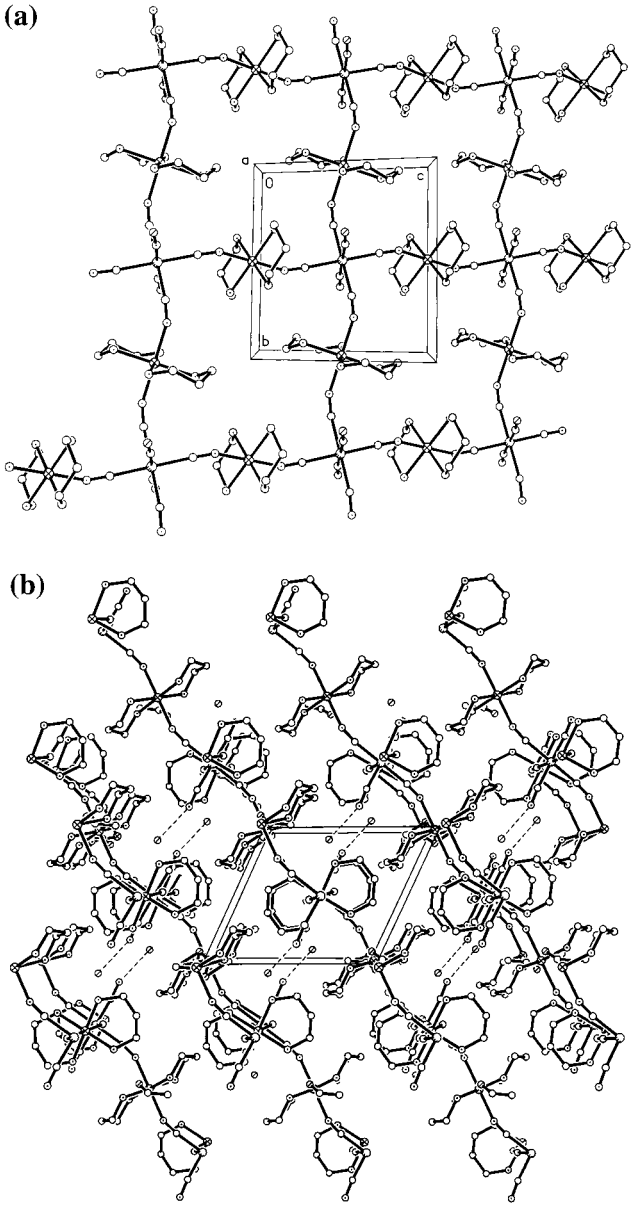

Figure 2. Projections showing (a) a 2-D layer of complex **1** and (b) the stacking of layers.

Table 3. Selected Bond Lengths (Å) and Angles (deg) for Complex **2**

Co−C(2)	1.894(5)	Co−C(3)	1.904(6)
Co−C(1)	1.901(5)	Ni(1)−N(5)	2.102(5)
Ni(1)−N(1)	2.145(5)	Ni(1)−N(4)	2.127(5)
Ni(2)−N(7)	2.109(5)	Ni(2)−N(6)	2.107(5)
Ni(2)−N(2)	2.155(4)		
C(1)−N(1)−Ni(1)	148.2(4)	C(2)−N(2)−Ni(2)	153.9(4)
N(1)−C(1)−Co	172.4(5)	N(2)−C(2)−Co	174.2(5)
N(3)−C(3)−Co	174.8(5)		

anion coordinates to four adjacent *trans*-$[Ni(tn)_2]^{2+}$ cations through four cyano nitrogens (N(1), N(1)#1, N(2), N(2)#2) in a plane with Ni−N distance of 2.145(5) for Ni(1)−N(1) and 2.155(4) Å for Ni(2)−N(2). The Ni−N≡C bond angles range from 148.2(4)° to 153.9(4)°, i.e., the bridging CN ligands coordinate to Ni(II) ions in a bent fashion as in complex **1**. The distances between nearest metal centers are 4.931 Å for Co···Ni(1), 5.032 Å for Co···Ni(2) and 7.283 Å for Ni(1)···Ni(2). The NO_3^- counteranion is situated within the holes of the $\{Ni-C\equiv N-Co\}_4$ basic units of the grid and hydrogen-bonded to N(7)

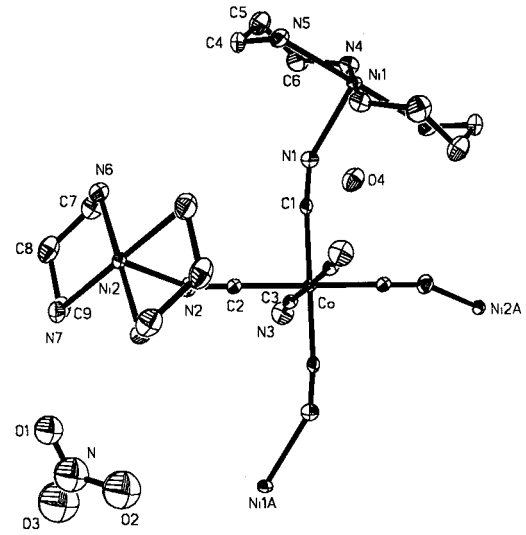

Figure 3. ORTEP view of complex **2** with atom numbering scheme showing 30% probability ellipsoids (hydrogen atoms are omitted for clarity).

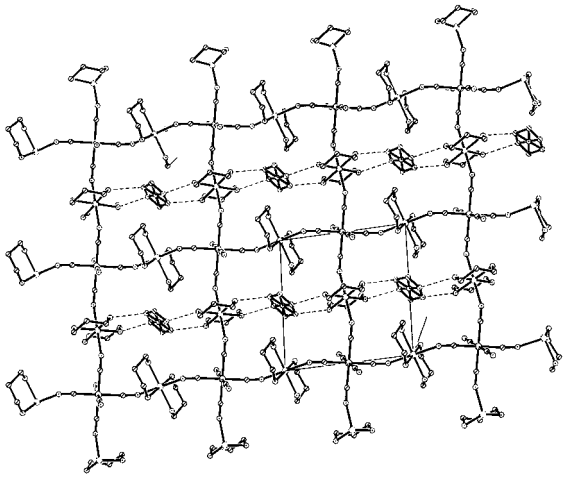

Figure 4. Projection showing a 2-D layer of complex **2**.

of the tn ligand (O(1)···N(7), 2.958 Å and O(3)#3···N(6), 2.842 Å). The water molecules are located between the sheets and hydrogen-bonded to the terminal CN ligand of $Co(CN)_6^{3-}$ (O(4)···N(3)#4, 2.837 Å) and to the coordinating tn ligand (N(4)···O(4), 3.102 Å). The shortest interlayer metal−metal distance is 8.937(2) Å for Ni(1)···Ni(1) and Ni(2)···Ni(2) (cell dimension *a*).

Magnetic Properties. The magnetic susceptibility of **1** has been measured in the 1.8−300 K temperature range. A plot of $\chi_M T$ vs T is shown in Figure 5, where χ_M is the magnetic susceptibility per Ni_2Cr unit. $\chi_M T$ increases slowly with decreasing temperature, down to ca. 40 K and then sharply, reaching a maximum value of 8.8 emu K mol^{-1} (8.4 μ_B) at 6.5 K. The $\chi_M T$ value (3.0 emu K mol^{-1}, 4.90 μ_B) at room temperature is higher than expected for the spin-diluted $S_T = 2 \times 1+1/2$ system (2.38 emu K mol^{-1} with $g = 2.0$). The maximum value, much larger than the spin-only value of 4.38 emu K mol^{-1} (5.92 μ_B) for $S_T = 2.5$, results from the ferromagnetic interactions between two nickel(II) ions ($S = 1$, $g = 2.0$) and one low-spin chromium(I) ion ($S = {}^1/_2$, $g = 2.0$),[41] suggesting the occurrence of magnetic ordering. Below 6.5 K, $\chi_M T$ decreases rapidly, due to interlayer antiferromagnetic interactions (Vide infra). The

(41) Manoharan, P. T.; Gray, H. B. *J. Am. Chem. Soc*. **1965**, *87*, 3340.

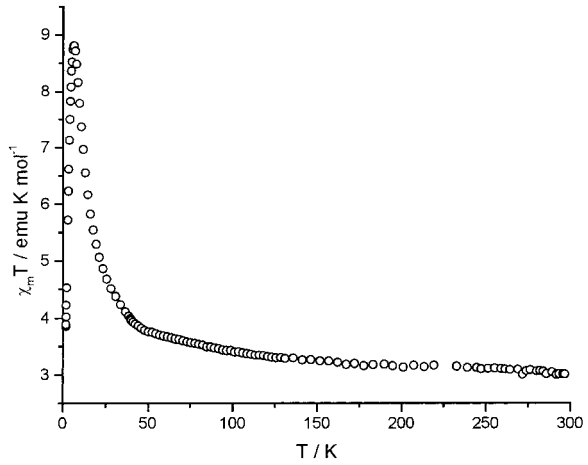

Figure 5. Temperature dependence of $\chi_M T$ for complex **1**.

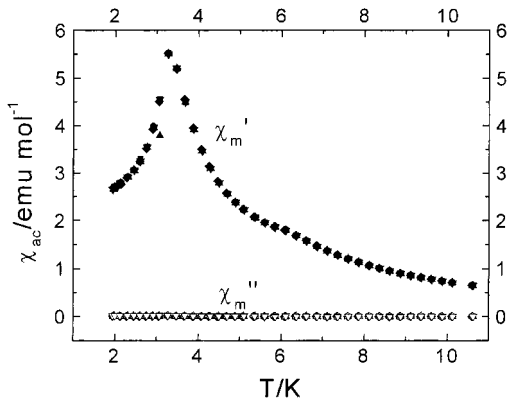

Figure 6. Real, χ, and imaginary χ ac magnetic susceptibility as a function of temperature taken at 133, 199, 355, 633, and 1111 Hz for complex **1**.

magnetic susceptibility above 10 K obeys the Curie−Weiss law with a positive Weiss constant = +11.5 K, which also supports the presence of ferromagnetic interactions within the $\{Cr(-C\equiv N-Ni)_2\}_n$ grid-like layers of **1**.

The onset of a magnetic phase transition is further confirmed by the temperature dependence of the ac molar magnetic susceptibility displayed in Figure 6. The real part of the zero field ac magnetic susceptibility possess a maximum at ca. 3.3 K for frequencies of 133, 199, 355, 633, and 1111 Hz, and the imaginary part (χ_m'') is negligibly small, evidencing antiferromagnetic ordering below 3.3 K.[42]

The magnetization (0−6 T) measured at 1.93 K is shown in Figure 7 in the form of $M/N\mu_B$ (per Ni_2Cr unit) vs H, where M, N, μ_B, and H are magnetization, Avogadro's number, the electron Bohr magneton, and applied magnetic field, respectively. The magnetization increases rapidly reaching a value of 4.78 $N\mu_B$ at 6 T which is close to the saturation value of 5 $N\mu_B$ expected for the Ni_2Cr system ($S = 2.5$), which indicates the presence of ferromagnetic interactions between adjacent Cr^{I} and Ni^{II} ions.

The −0.2 to +0.2 to −0.2 T loop (Figure 8) shows no appreciable hysteresis at 1.93 K. The magnetic field dependence has a marked sigmoidal shape, suggesting a metamagnetic behavior. The magnetization first increases slowly with increasing magnetic field and then sharply showing a spin-flip from antiferromagnetic to ferromagnetic arrangement between the layers. The critical field (lowest field needed to reverse the interlayer antiferromagnetic interaction) is ca. 500 G at 1.93 K.

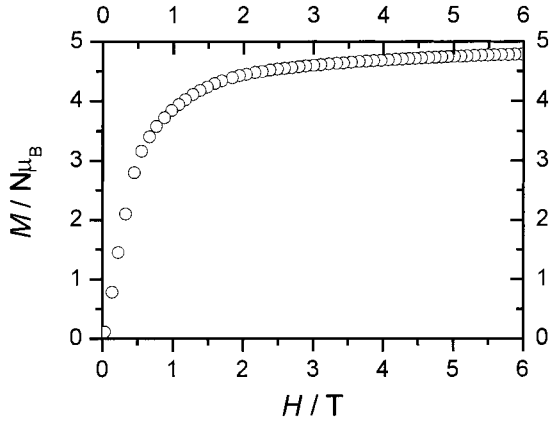

Figure 7. Magnetization curve at 1.93 K for complex **1**.

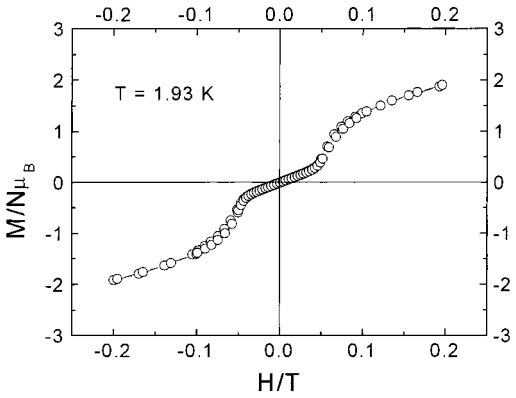

Figure 8. Magnetic field dependence of the magnetization in the −0.2, +0.2, −0.2 T loop at 1.93 K for complex **1**.

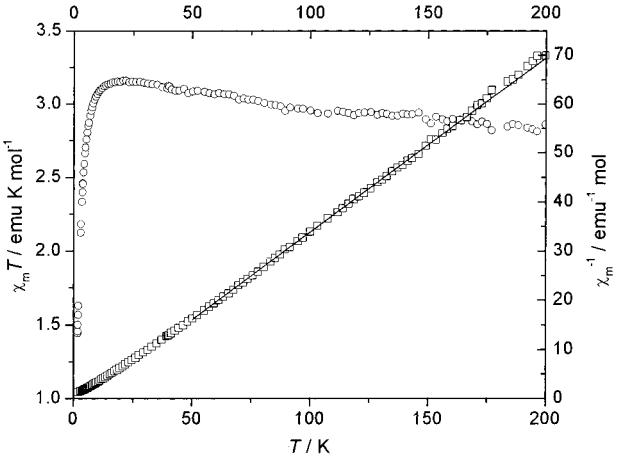

Figure 9. Temperature dependences of $\chi_M T$ and χ_M-1 for complex **2**. The solid line represents the best fit to the Curie−Weiss expression.

The magnetic susceptibility of complex **2** has been measured in the 1.8−200 K temperature range. A plot of $\chi_M T$ vs T is shown in Figure 9, where χ_M is the magnetic susceptibility per Ni_2Co unit. The $\chi_M T$ value increases smoothly on lowering the temperature down to ca. 17 K, reaching a maximum value of 3.15 cm^3 K mol^{-1}. Below 17 K, $\chi_M T$ decreases rapidly down to 1.8 K. This magnetic behavior is characteristic of a dominant ferromagnetic interaction with superimposition of weak antiferromagnetic interactions. The magnetic susceptibility has been fitted with the Curie−Weiss expression in the 50−200 K temperature range, as usually done for weakly coupled systems. A positive Weiss constant $\theta = +5.0$ K and $g_{Ni} = 2.37$ have

(42) Goodenough, J. B. *Phys. Rev.* **1955**, *100*, 564.

been obtained, suggesting the presence of an overall ferromagnetic behavior. The deviation from the Curie−Weiss expression at low temperatures confirms the presence of weak antiferromagnetic interactions.

Discussion

The reaction of $K_3[M(CN)_6]$ (M = Cr, Fe, Co) with $[Ni(diamine)_3]^{2+}$ (diamine = ethylenediamine, 1,2-propanediamine, 1,1-dimethylethylenediamine, 1,3-propanediamine) could give rise to two different bimetallic assemblies: (1) 1-D chainlike complexes $[Ni(diamine)_2]_3[M(CN)_6]_2$ possessing cyano-bridged neutral Ni_3M_2 chains;[16] (2) 2-D grid-like species $[Ni(diamine)_2]_2[M(CN)_6]X$ (X = NO_3^-, N_3^-, ClO_4^-, I^-, etc.) containing polymeric cation and the counteranion X.[22,24] In the absence of suitable counteranions, the former assemblies are obtained. This indicates that the counteranion serves as a template to help construct the 2-D grid-like network. The presence of excessive diamine usually gives crystalline complexes. This method has been adopted to prepare the present complexes. In the case of complex **1**, almost 10:1 molar ratio of tn:Ni was taken to avoid rapid precipitation of **1**.

The ferromagnetic interaction between chromium(I) and nickel(II) is due to the strict orthogonality of the magnetic orbitals of the low-spin Cr(I) [d,[5] $(3d_{xy})^1$] and Ni(II) [d,[8] $(d_{x^2-y^2})^1(d_{z^2})^1$] ions.[26b]

It is of interest to compare the magnetic properties of **1** and $[NiL]_3[Cr(CN)_5(NO)]_2\cdot 10H_2O$.[26b] The structural data show that the Ni-bridging cyano nitrogen bond distance (2.123(2)−2.144(3) Å) in the latter compound is much larger than in the former (2.083 Å). A long bond distance is unfavorable for magnetic coupling, which is in good agreement with the difference in Weiss constants (+10.0 K for $[NiL]_3[Cr(CN)_5(NO)]_2\cdot 10H_2O$). The small hysteretic field is typical of a soft magnet and ascribed to small magnetic anisotropy as well as the absence of irreversible movements of domain walls.[33b]

The origin of ferromagnetic interactions in complex **2** is intriguing. It may be due to a σ-superexchange between nearest intralayer nickel(II) (or Ni^{II}) ions ($t_{2g}^6e_g^2$) through the empty d_σ orbital of the cobalt(III) (or Co^{III}) ion (t_{2g}^6). On this basis, an electron spin of the same sign as that of the unpaired electron on the d_{z^2} orbital (paramagnetic Ni^{II}) is polarized on the d_{z^2} orbital (diamagnetic Co^{III}) through the filled orbital of the cyanide bridge (the *z* axis is taken along the Ni−C≡N−Co linkage), giving rise to a ferromagnetic interaction between the nearest intrachain paramagnetic nickel(II) ions. This mechanism, first suggested by Goodenough,[42] has been recently considered for explaining the three-dimensional ferromagnetic interactions in $[Ni(en)_2]_3[Fe^{II}(CN)_6]PF_6$ and $[Ni(tn)_2]_3[Fe^{II}(CN)_6]X_2$ (X = PF_6^- or ClO_4^-).[33d] According to this mechanism, the chainlike $[Ni(en)_2]_3[Co(CN)_6]_2\cdot 2H_2O$[16b] and $[PPh_4][Ni(pn)_2][Co(CN)_6]$[16c] complexes should exhibit intrachain ferromagnetic interactions. The overall antiferromagnetic interaction observed in these complexes is likely to result from the predominancy of interchain antiferromagnetic interactions over weak intrachain ferromagnetic interactions. At this stage, it is worth mentioning that complete dehydration of the one-dimensional $[Cu(dien)]_3[Fe(CN)_6]_2\cdot 6H_2O$ chain complex results in a dramatic modification of its overall magnetic behavior, which changes from ferromagnetic to antiferromagnetic.[18c] The intramolecular ferromagnetic interaction due to the strict orthogonality of magnetic orbitals of copper(II) and low-spin iron(III) within the Cu_2Fe chain,[18a] is not modified by dehydration, whereas the interchain magnetic interaction (usually antiferromagnetic) becomes stronger upon dehydration. This results in an overall antiferromagnetic interaction for the dehydrated complex. This observation adds support to our above interpretation.

Conclusions

$[Ni(tn)_2]_2[Cr(CN)_5(NO)]OH$ (**1**) and $[Ni(tn)_2]_2[Co(CN)_6]NO_3\cdot 2H_2O$ (**2**) bimetallic assemblies possess a two-dimensional grid-like molecular structure. Magnetic studies showed that long-range antiferromagnetic ordering was observed at $T_N = 3.3$ K. Below T_N, complex **1** displays a metamagnetic behavior originating from intralayer ferromagnetic and interlayer antiferromagnetic interactions. This result supports the conclusion drawn by Ohba et al. that metamagnetism occurs when the interlayer separation is small enough to allow strong enough antiferromagnetic interactions.[22] The T_N values appear to be related to the strength of the interlayer antiferromagnetic interactions. Complex **2** exhibits intramolecular $Ni^{II}\cdots Ni^{II}$ ferromagnetic interactions through the diamagnetic $-N\equiv C-Co^{III}-C\equiv N-$ pathways, which can be explained by superexchange through the empty d_σ orbitals of the diamagnetic cobalt(III) ion. The present study shows that these ferromagnetic interactions may be commonly present in cyano-bridged Ni(II)−Co(III) bimetallic assemblies.

Acknowledgment. The National Natural Science Foundation of China (No. 20071019 and No. 20071020) and CNRS are acknowledged for support of this work through the CNRS/NSFC exchange program.

Supporting Information Available: The X-ray crystallographic file in CIF format. This material is available free of charge via the Internet at http://pubs.acs.org.

IC0013330